Pergamon

PII: S0306-4522(97)00692-1

Neuroscience Vol. 85, No. 4, pp. 1195–1208, 1998

0306-4522/98 $19.00+0.00

COHERENCE ANALYSIS OF THE HUMAN SLEEP ELECTROENCEPHALOGRAM

P. ACHERMANN* and A. A. BORBÉLY

Institute of Pharmacology, University of Zürich, Winterthurerstrasse 190, CH-8057 Zürich, Switzerland

Abstract—Animal studies have shown that the sleep-related oscillations in the frequency range of spindles and slow-waves, and in the gamma band occur synchronously over large parts of the cerebral cortex. Coherence analysis was used to investigate these oscillations in the human sleep electroencephalogram. In all-night electroencephalogram recordings from eight young subjects power and coherence spectra within and between cerebral hemispheres were computed from bipolar derivations placed bilaterally along the antero-posterior axis. The 0.75–50 Hz range was examined with a resolution of 0.25 Hz. Distinct peaks in coherence were present in non-rapid eye movement sleep but not in rapid eye movement sleep. The most prominent and consistent peak was seen in the range of sleep spindles (13–14 Hz), and additional peaks were present in the alpha band (9–10 Hz) and low delta band (1–2 Hz). Whereas coherence in the spindle range was highest in stage 2, the alpha peak was most prominent in slow-wave sleep (stages 3 and 4). Interhemispheric coherence at 30 Hz was higher in rapid eye movement sleep than in non-rapid eye movement sleep. There were also marked sleep state-independent regional differences. Coherence between homologous interhemispheric derivations was high in the low frequency range and declined with increasing frequencies, whereas coherence of intrahemispheric and non-homologous interhemispheric derivations was at a low level throughout the spectra.

It is concluded that coherence analysis may provide insights into large-scale functional connectivities of brain regions during sleep. The high coherence of sleep spindles is an indication for their widespread and quasi-synchronous occurrence throughout the cortex and may point to their specific role in the sleep process. © 1998 IBRO. Published by Elsevier Science Ltd.

Key words: alpha activity, coherence, human sleep, non-REM sleep, REM sleep, sleep spindles.

The changes of electroencephalogram (EEG) amplitude and frequency during sleep are used as the main criteria for discriminating the two sleep states non-rapid eye movement (REM) sleep and REM sleep, and for subdividing human non-REM sleep into four stages.[42] Quantitative analysis of the sleep EEG has been useful for demonstrating that slow-wave activity (SWA, power in the 0.75–4.5 Hz range) and spindle frequency activity (SFA, power in the 12–15 Hz range) are markers of processes underlying sleep regulation. Thus SWA is typically high in the first non-REM sleep episode and declines over subsequent episodes.[12,21] Moreover, it has been shown that its initial level is determined by the duration of prior waking and sleep.[12,22,57] SWA has served for delineating the time-course of the homeostatic Process S in the two-process model of sleep regulation.[2,10,11,19] In contrast to SWA, SFA is determined by both homeostatic and circadian factors.[4,20] Within non-REM sleep episodes, SFA peaks earlier than SWA and shows partly an inverse relationship to SWA.[3,23]

Recent advances in the neurophysiology of sleep-related processes showed that SWA and SFA can be related to changes at the cellular level. The progressive hyperpolarization of thalamocortical neurons which occurs with the progression from waking to deep non-REM sleep,[29] engenders fluctuations in the membrane potential in the frequency range of the sleep EEG.[46,50] At a moderate level of hyperpolarization oscillations occur in the range of sleep spindles, whereas at a high level they are in the delta range (0.75–4.5 Hz). Therefore the progression from "spindle sleep" (stage 2) to slow-wave sleep (stages 3 and 4), and the partly inverse relationship between EEG power density in the spindle and slow-wave ranges in humans[3] have a counterpart at the level of thalamocortical neurons. Also fluctuations at the cellular level at frequencies below 1 Hz were recently shown to have a complement in the human sleep EEG.[1,6] Spindles are characterized by their synchronous occurrence in different cortical areas.[45] This synchronization is due to the divergent connectivity of corticothalamic networks as well as to the synchronized slow oscillations over large cortical territories which trigger thalamic reticular cells nearly simultaneously.[17,18] Of importance is the reticular

*To whom correspondence should be addressed.

Abbreviations: CSD, current source density; EEG, electroencephalogram; EMG, electromyogram; EOG, electrooculogram; MEG, magnetencephalogram; REM, rapid eye movement; SFA, spindle frequency activity (EEG power in the 12–15 Hz range); SWA, slow-wave activity (EEG power in the 0.75–4.5 Hz range); SWS, slow-wave sleep.

nucleus since its isolation abolished spindles in the cortex and the deafferented nucleus itself could generate spindle oscillations.[46] One of the questions addressed by the present study was whether the widespread, synchronous occurrence of spindles is evident also in scalp recordings of the human EEG.

History related, regional changes in the sleep EEG have been recently observed. Thus a prolonged sensory stimulation of the dominant hand prior to sleep enhanced the low-frequency components of the sleep EEG in the derivation overlying the contralateral somatosensory cortex.[32] Moreover, in regular sleep recordings of young adults, SWA in the initial part of sleep was more prominent at an anterior derivation (F3C3) than at more posterior derivations (C3P3, P3O1), a difference that vanished with the progression of sleep.[55,56] Also this observation may reflect a history-related regional change in the sleep EEG, since frontal cortical areas are known to be particularly involved in waking activities. Taken together, the results support the notion that sleep has a local, use-dependent component in addition to being a global brain phenomenon.[9,34]

The aim of the present study was to extend the topographic analysis of the sleep EEG by examining the functional connectivities between brain regions. Coherence, a correlation measure in the frequency domain, has proved to be a useful measure. In clinical applications, coherence has been shown to reveal damage to fibres in the periventricular white matter as quantified by magnetic resonance imaging.[37] Although the coherence analysis has been applied to the sleep EEG, there were methodological limitations rendering the interpretation of the data difficult. These include the restriction of the analysis to selected, short segments of sleep EEG,[24,39] the use of a small number of derivations,[8] and montages with a common reference electrode which introduce a potential bias in the coherence data[7,25,39,52] (for a discussion of the problem, see Refs 27 and 36). Whereas many of these problems were overcome in a recent study,[31] the data analysis was not based on a high frequency resolution. In the present study, we computed coherence over a large frequency range with a high frequency resolution. A major question was whether state and site-specific functional connectivities would be revealed which could contribute to the understanding of sleep processes. Coherent gamma band activity during sleep has been recently reported by Llinás and Ribary[38] using magnetencephalogram (MEG) recordings and its possible functional role for REM sleep was discussed.

EXPERIMENTAL PROCEDURES

Subjects and data recording

Nocturnal sleep (sleep episode: 23.00–07.00) of eight healthy young right-handed men (mean age 23.5 years, range 22–26 years) was recorded after an adaptation night. A screening night served to exclude subjects with sleep apnea and nocturnal myoclonus. The subjects reported to be in good health and free of sleep complaints. They were instructed to abstain from caffeine and alcohol and to keep a regular sleep–wake schedule for at least seven days prior to the study. Compliance with the instructions was verified by inspecting the ambulatory wrist activity recording during the week preceding the study, and determining the concentration of caffeine in saliva and of alcohol in breath prior to the experimental night. Informed written consent was obtained from the subjects.

The electroencephalogram (EEG; F3, P3, O1, F4, C4, P4, O2, and A2, all against C3), the submental electromyogram (EMG), the electrooculogram (EOG, differential recording), and the electrocardiogram were recorded by a polygraphic amplifier (PSA 24, Braintronics, The Netherlands), digitized, and transmitted via a fibre optic link to a personal computer with a digital signal processor board. After analogue signal conditioning (high-pass filter -3 dB at 0.16 Hz; low-pass filter -3 dB at 102 Hz, < -40 dB at 256 Hz; notch filter at 50 Hz), the signals were sampled at 512 Hz, digitally filtered (EEG: low-pass FIR filter, -3 dB at 49 Hz; EMG: band-pass FIR filter, -3 dB points 15.6 and 54 Hz) and stored with a resolution of 128 Hz.

One of the subjects was studied for an additional night with a portable 32 channel system (Nihon Kohden Neurofile II, Japan). Twenty-nine EEG channels (including mastoids) with electrode positions according to an extended 10–20 system, an EMG and a bipolar EOG were recorded. Data were sampled with 256 Hz, digitally filtered (low-pass FIR filter, -3 dB at 40 Hz) and stored with a resolution of 128 Hz.

Sleep stage scoring and signal analysis

Sleep stages were visually scored for 20 s epochs (C3A2 derivation) according to the criteria of Rechtschaffen and Kales.[42] Only 20 s epochs without artifacts were used for further analysis. To avoid coherent activity due to contamination by eye movements, REM sleep epochs with rapid eye movements were also excluded. They were visually identified when an EOG deflection unrelated to an EEG event showed a peak-to-peak amplitude of ≥ 75 μV and a slope of ≥ 200 μV/s. Power spectra of consecutive 20 s epochs (fast Fourier transform routine, Hanning window, averages of five 4 s epochs) were computed for the bipolar derivations F3C3, P3O1, F4C4, P4O2, and coherence spectra (20 s epochs) within and between hemispheres were calculated using Welch's averaged periodogram method[54] (five 4 s epochs). The frequency resolution was 0.25 Hz and frequencies up to 50 Hz were analysed. The two lowest frequency bins (0.25 and 0.5 Hz) were excluded from the analysis because of numerous low-frequency artifacts (due to sweating, etc.). The artifact free database would have been too restricted for a meaningful analysis.

The squared coherence spectrum function C_{xy} for the two signals x and y is defined as:

$$C_{xy} = P_{xy}(f)^2/(P_{xx}(f) \cdot P_{yy}(f))$$

with f denoting frequency and P power or cross-power. Before computing averages, Fisher's z-transformation was applied to the coherence values (square root of above defined values) which yielded an identical variance for all frequency bins.[41] Re-transformed and squared coherence spectra are plotted in all the figures and referred to as coherence spectra.

For the night recorded with the 32 channel system, the coherence spectra of current source density approximations (CSD)[30,53] FC1 – PO1 and FC2 – PO2 were computed. For example for the derivation FC1 the CSD approximation was defined as:

$$\text{CSD}\ FC1 = [(FC1 - F3) + (FC1 - FZ) + (FC1 - CZ) + (FC1 - C3)]^{\frac{1}{2}}$$

Table 1. Sleep measures derived from visual scoring

Sleep onset latency	9.4	(3.1)
REM sleep latency	74.3	(6.6)
Total sleep time	458.0	(2.3)
Waking	14.6	(2.4)
Stage 1	42.1	(5.3)
Stage 2	219.1	(10.9)
Stage 3	51.8	(5.5)
Stage 4	41.9	(10.3)
SWS (Stages 3+4)	93.7	(11.0)
REM sleep	103.1	(6.3)
Movement time	7.1	(0.9)

Mean values (S.E.M.; n=8) in minutes.
Sleep onset latency: latency from lights off to first occurrence of stage 2.
REM sleep latency: latency from sleep onset to first occurrence of REM sleep.

CSD reveals the component perpendicular to the surface of the head and therefore accentuates the contribution of the potential field under the active electrode relative to the surrounding field.

Signal analysis and statistics were performed with the software package MATLAB and its signal analysis and statistics toolbox (The Math Works, Inc., U.S.A.). *Post hoc* two-tailed paired t-tests were only performed if an appropriate ANOVA for repeated measures revealed a significant effect of factor "derivation" or "state". Care has to be taken in interpreting the statistics of multiple comparisons. Since adjacent frequency bins do not vary independently, a Bonferroni correction for 198 bins would be too conservative. We therefore plot the P-values themselves below the 0.05 level so that the degree of significance is evident to the reader.

RESULTS

Sleep measures derived from visual scoring

The sleep measures were typical for healthy young subjects (Table 1).

Power and coherence spectra in different sleep stages (individual data)

Figure 1 provides an example of two 20 s stage 2 recordings from an anterior and posterior bipolar derivation with the corresponding power and coherence spectra. Sleep spindles which are present in the bottom recording give rise to a distinct 14 Hz peak in the power and coherence spectra.

Figure 2 contrasts average intrahemispheric and interhemispheric power and coherence spectra of an individual in different sleep stages. The power spectra plotted on a logarithmic scale show the typical decreasing trend from low to high frequencies. A peak at 13.5–13.75 Hz, the frequency of sleep spindles, is present in stage 2 and slow-wave sleep (SWS). An additional peak at 9.0 Hz is seen in SWS. Power in the lowest frequency band is at a maximum in SWS. There is a minor peak in the theta band at 6.75 or 8.0 Hz in both stage 1 and REM sleep.

In contrast to the power spectra, the level of intrahemispheric coherence (Fig. 2, left panels) exhibits no prominent frequency-dependent trend. In stage 1 and REM sleep, the values are at a low level throughout the spectrum. In stage 2, the large 14 Hz peak is the distinguishing feature. It is smaller in SWS where an additional peak in the alpha band is present. Coherence in the lowest frequencies shows a moderate elevation in stage 2 and SWS.

The spectra of interhemispheric coherence (Fig. 2, right panels) differ from those of intrahemisperic coherence. The level is higher at the low end of the spectrum and there is a frequency-dependent decline up to 20 Hz. The alpha and spindle peaks appear to be superimposed upon this pattern. The alpha peak in SWS is larger than in the intrahemispheric spectrum. Moreover, there is a minor theta peak in stage 1 and REM sleep.

Random level of coherence

To determine the random level of coherence, the records from two derivations were shifted by 20 s relative to each other. The resulting spectra showed an average coherence level of 0.1815 for the data of the individual represented in Fig. 2, and a mean value of 0.1829 (S.E.M.=0.0013) for the eight subjects.

Interindividual variability of coherence in the sigma band

The most prominent feature of the coherence spectra in stage 2 was the peak in the frequency range of sleep spindles. As shown in Fig. 3 it was a consistent feature in all individuals. Although there was some variability in the peak amplitude of left and right intrahemispheric coherence (left two columns), there was no statistically significant lateralization. In the anterior interhemispheric spectra, the spindle peak was prominent in all individuals, whereas at the posterior sites it was attenuated or absent.

Non-rapid eye movement sleep versus rapid eye movement sleep (mean data)

The mean coherence spectra for non-REM sleep (stages 2, 3 and 4; Fig. 4) and REM sleep (Fig. 5) were calculated for derivations within the same hemisphere as well as for homologous and non-homologous derivations between hemispheres.

The main features described for the individual in Fig. 2 were also present in the mean data. The intrahemispheric coherence spectra showed a flat, low-level spectrum with a dominant spindle peak, a small alpha peak and an elevation in the low delta band. In REM sleep, the peaks were absent. Interhemispheric coherence of the homologous anterior derivations exhibited in non-REM sleep distinct low-delta, alpha and spindle peaks superimposed on the marked declining trend from low to high frequencies. The spectrum of the homologous posterior derivations was similar but the alpha and spindle peaks

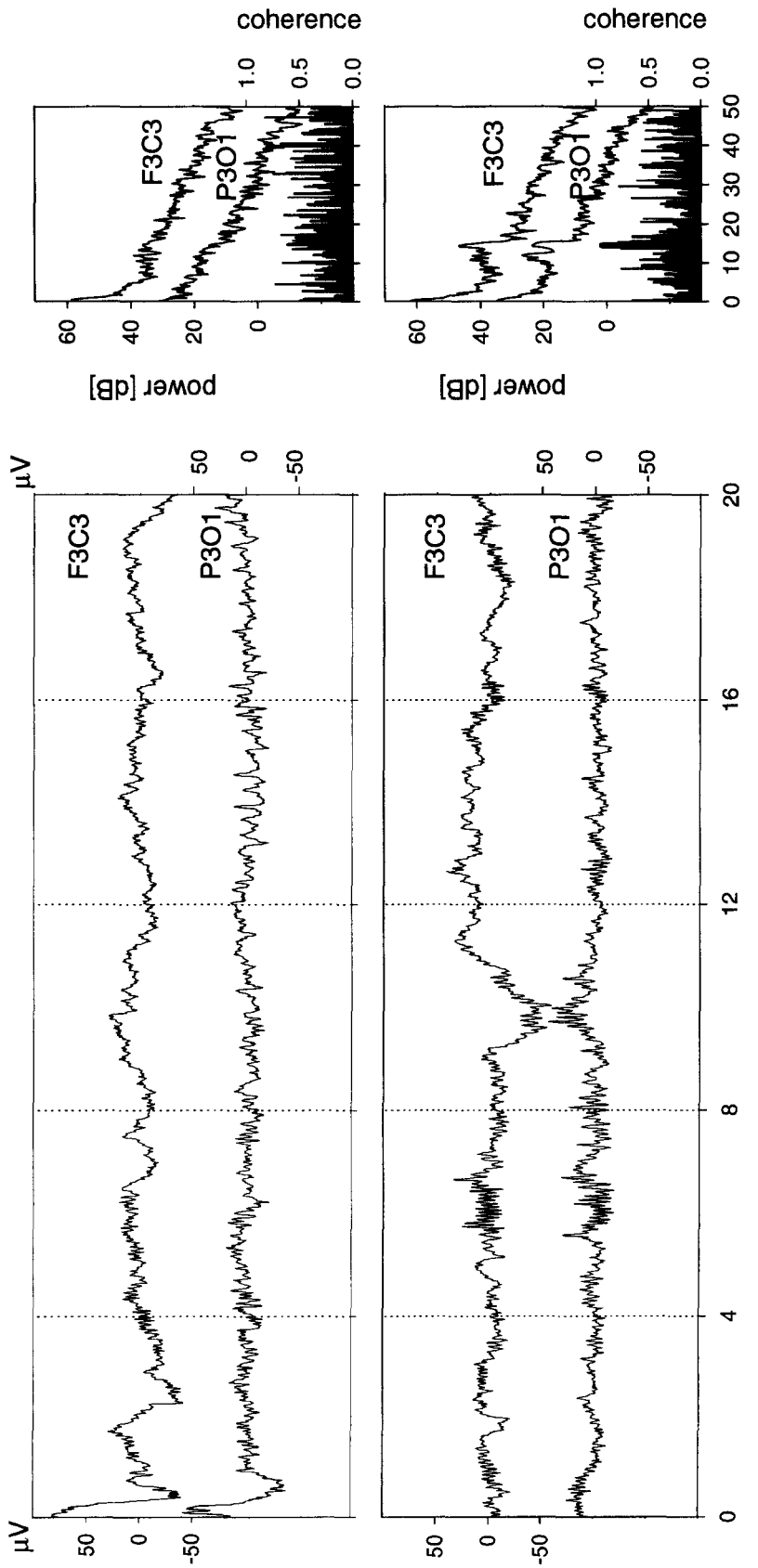

Fig. 1. 20 s EEG recordings of stage 2 for two different derivations (F3C3, P3O1), the corresponding power spectra (average of five 4 s epochs), and the coherence spectra (F3C3 – P3O1). Sleep spindles are present in the lower recording. Power spectra are plotted on a logarithmic scale (0 dB=1 μV^2/0.25 Hz), and the spectra of the F3C3 derivation are displaced by +20 dB to facilitate visualization.

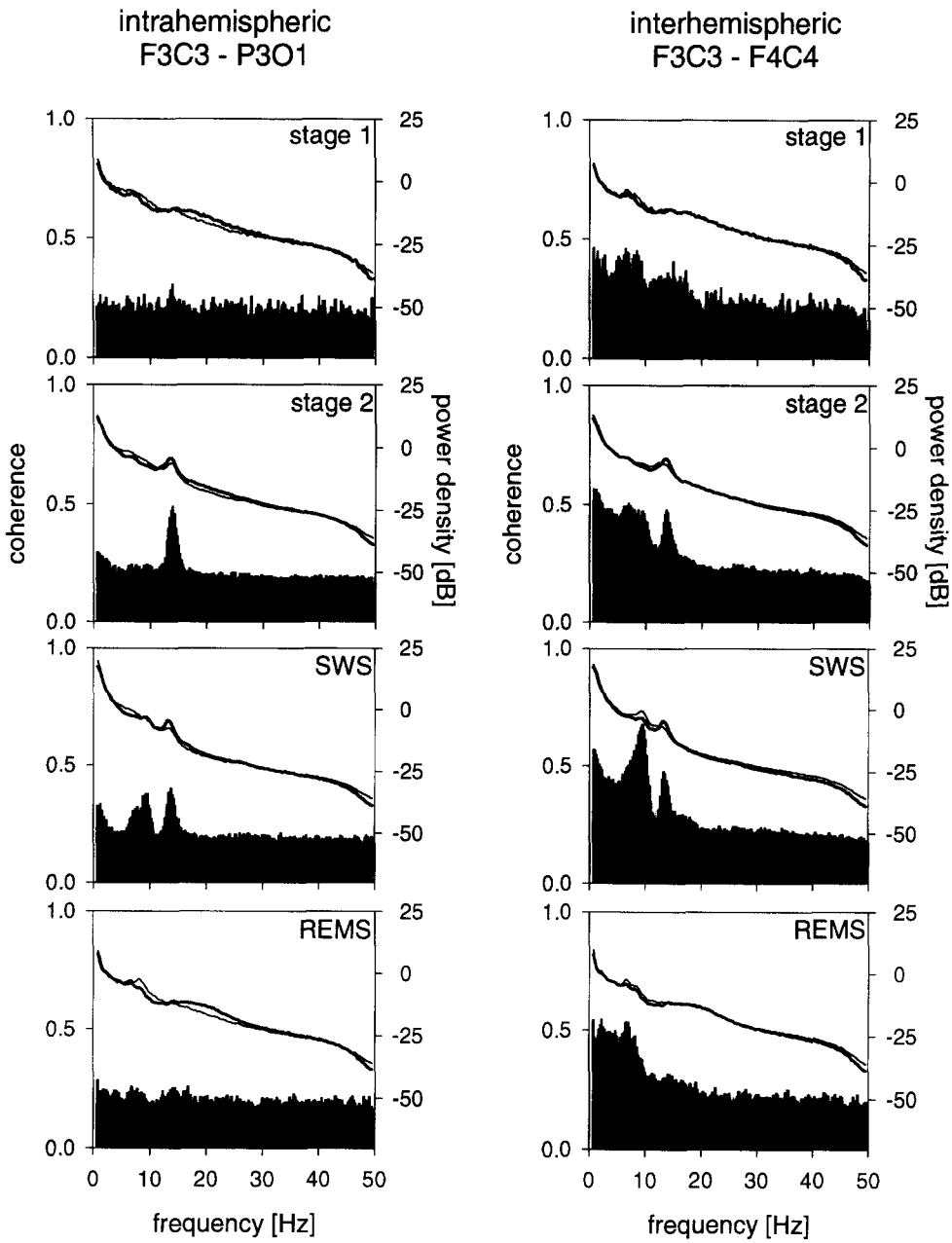

Fig. 2. Difference of power and coherence in different sleep stages. Average power spectra from two different derivations and the corresponding intrahemispheric (left) and interhemispheric coherence spectra (right) of an individual. Power spectra: Left, F3C3 thick line, P3O1 thin line; right, F3C3 thick line, F4C4 thin line. Stage 1, 49 20 s epochs; stage 2, n=514; slow-wave sleep (SWS), n=397; REM sleep (REMS), n=153. Power spectra are plotted on a logarithmic scale (0 dB=1 μV^2/0.25 Hz).

were attenuated. The same pattern without peaks was seen in the corresponding REM sleep spectra (Fig. 5). Note that at the anterior site the delta peak was not situated at the lowest frequency bin.

Interhemispheric coherence spectra between non-homologous sites were similar to the intrahemispheric spectra but the spindle peak in non-REM sleep was significantly lower. Moreover, as indicated by the bottom bars, the random level was attained already at lower frequencies.

Intrahemispheric and interhemispheric coherence differed significantly over almost the entire frequency range in both non-REM sleep (P<0.01 up to 46.5 Hz) and REM sleep (P<0.01 up to 43 Hz; ANOVA for repeated measures with factor "derivation" and subsequent two-tailed paired t-tests on Fisher's z-transformed coherence values). There was no significant left-right difference of the intrahemispheric spectra. However, anterior and posterior interhemispheric spectra differed. In non-REM sleep, anterior

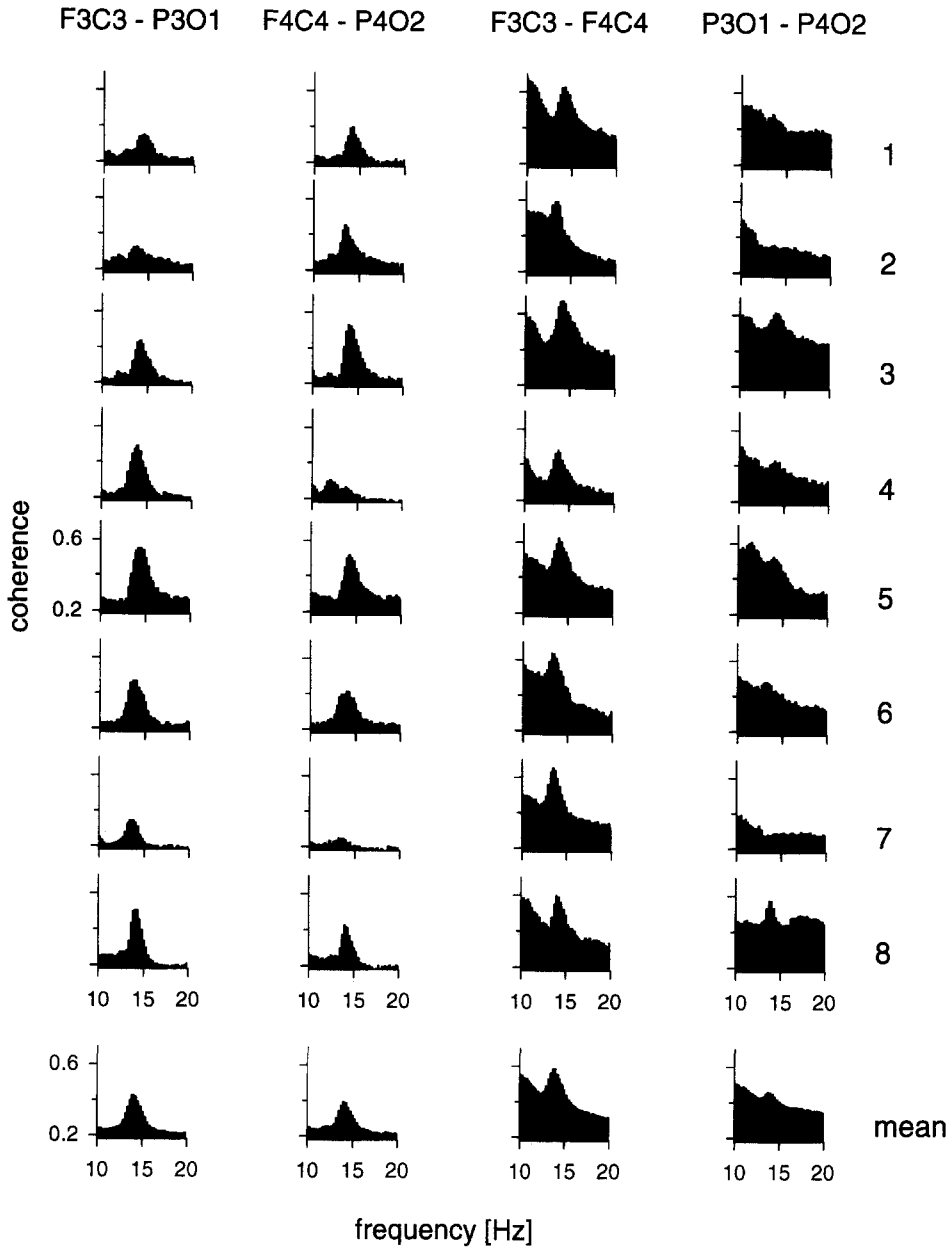

Fig. 3. Individual (1–8) and mean stage 2 coherence spectra in the 10–20 Hz range. Coherence was calculated within (F3C3 − P3O1, F4C4 − P4O2) and between hemispheres (F3C3 − F4C4, P3O1 − P4O2). On average 609.8 (12.2=S.E.M.) 20 s epochs contributed to a mean spectrum.

values dominated in the alpha (8.75–9.75 Hz, $P<0.05$) and spindle frequency range (13.75–14.75 Hz, $P<0.05$; 14.25 Hz, $P<0.01$), while posterior values were larger in the high delta/theta range (4.25–6.0 Hz, $P<0.05$; 4.75–5.5 Hz, $P<0.01$). In REM sleep, the anterior values were lower in the low delta band (0.75–1.5 Hz, $P<0.01$) and higher in some bins of the beta range (39.25–39.75 Hz, $P<0.05$; 39.75 Hz, $P<0.01$; 41.5–42.75, $P<0.05$; 42.5–42.75 Hz, $P<0.01$).

To examine the state-dependent differences in more detail, and to investigate changes within non-REM sleep, coherence in stage 2 (Fig. 6) and SWS (Fig. 7) were expressed relative to the corresponding REM sleep values. With this representation the sleep state-related changes can be viewed independently of the different basic coherence patterns. Power in non-REM sleep was also expressed relative to REM sleep (Fig. 8).

A progression of changes from stage 2 to SWS was evident. Although the spindle peak was in both stages a prominent feature, it was larger in stage 2. In contrast, the alpha peak was most conspicuous in SWS and emerged in stage 2 only in the anterior interhemispheric spectra. Finally, the elevation in the lowest delta bins was larger in SWS than in stage 2.

The spectra exhibited also marked regional differences. The spindle peak was largest in the

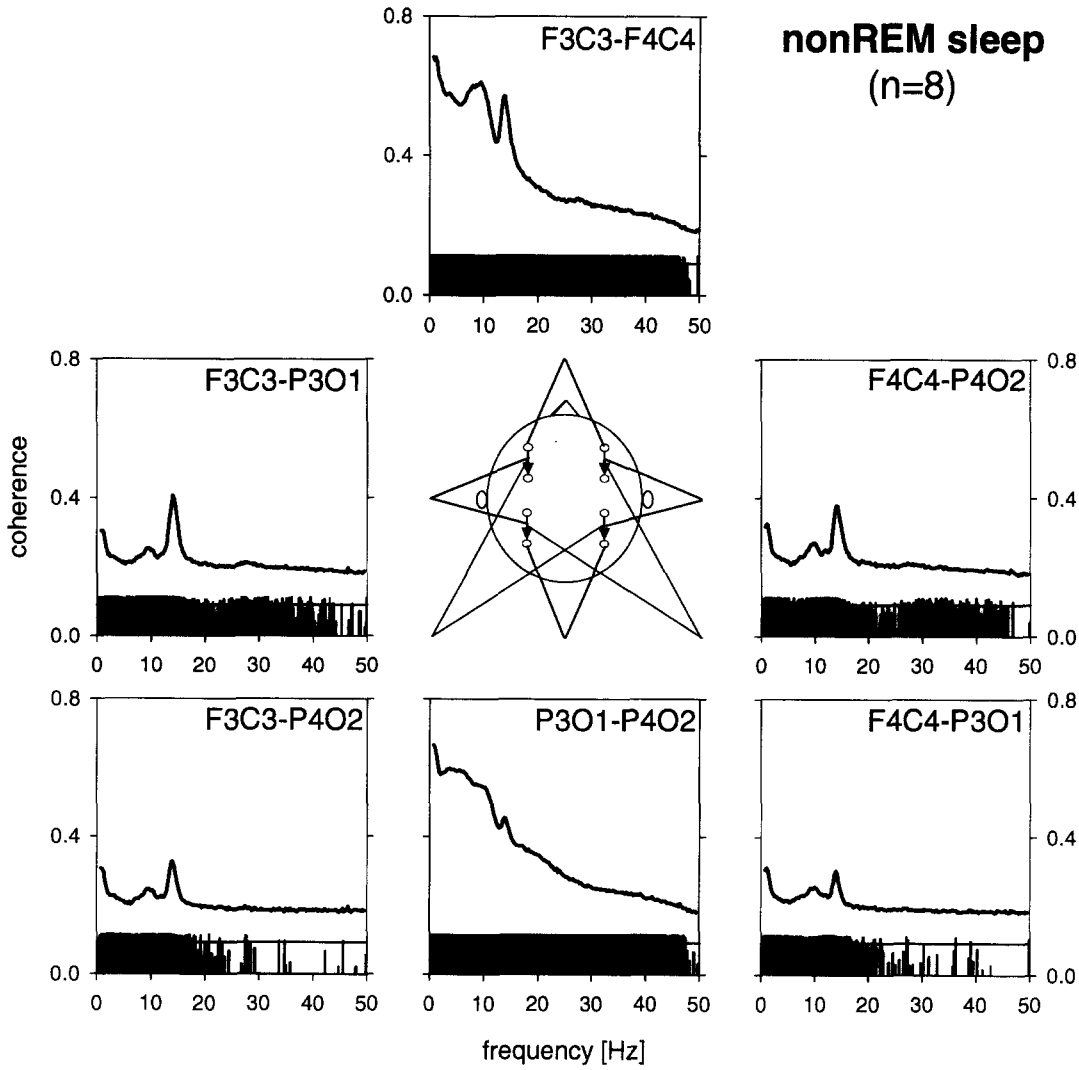

Fig. 4. Mean intrahemispheric and interhemispheric coherence spectra in non-REM sleep (stages 2 to 4) from eight subjects. Middle diagram indicates the pairs of bipolar derivations from which the spectra were calculated. On average 878.6 (7.4=S.E.M.) 20 s epochs contributed to a mean spectrum. Black bars above the abscissae indicate for each bin significant differences from random level of coherence (0.1829; only $P<0.05$ is shown; $1-P$ is plotted on a linear scale; the $P=0.01$ level is indicated by a horizontal line and $P=0.005$ corresponds to the abscissa; paired two-tailed t-tests on Fisher's z-transformed coherence values).

intrahemispheric spectra, the alpha peak in the interhemispheric spectra. The lowest modulation by non-REM sleep was seen in the posterior interhemispheric coherence. It is noteworthy that in the 1.5–3.75 Hz range ($P<0.05$; 1.75–3.0 Hz, $P<0.01$), the REM sleep values even exceeded those of SWS (Fig. 7).

Coherence in the high frequency range was almost invariably higher in REM sleep than in the two non-REM sleep stages. However, bins with significant differences were scattered and infrequent. They were more numerous in the interhemispheric spectra. A cluster around 30 Hz was seen in the interhemispheric SWS spectra and to lesser extent in the stage 2 spectra. Another cluster of significant bins was present between 39 and 45 Hz at the anterior interhemispheric site.

The pattern of the relative power spectra (non-REM sleep/REM sleep) was similar in the four derivations (Fig. 8). However, at the posterior sites the values deviated less from unity than at the anterior sites. At frequencies between 18 Hz and 43–48 Hz power was higher in REM sleep than in non-REM sleep.

Coherence spectra of current source density derivations

To test whether the pattern of the coherence spectra was specific for the bipolar derivation, computations were made for the same data for CSD derivations. CSD approximations were calculated for FC1, PO1, FC2, and PO2 in a subject (see Experimental Procedures). Only intrahemispheric

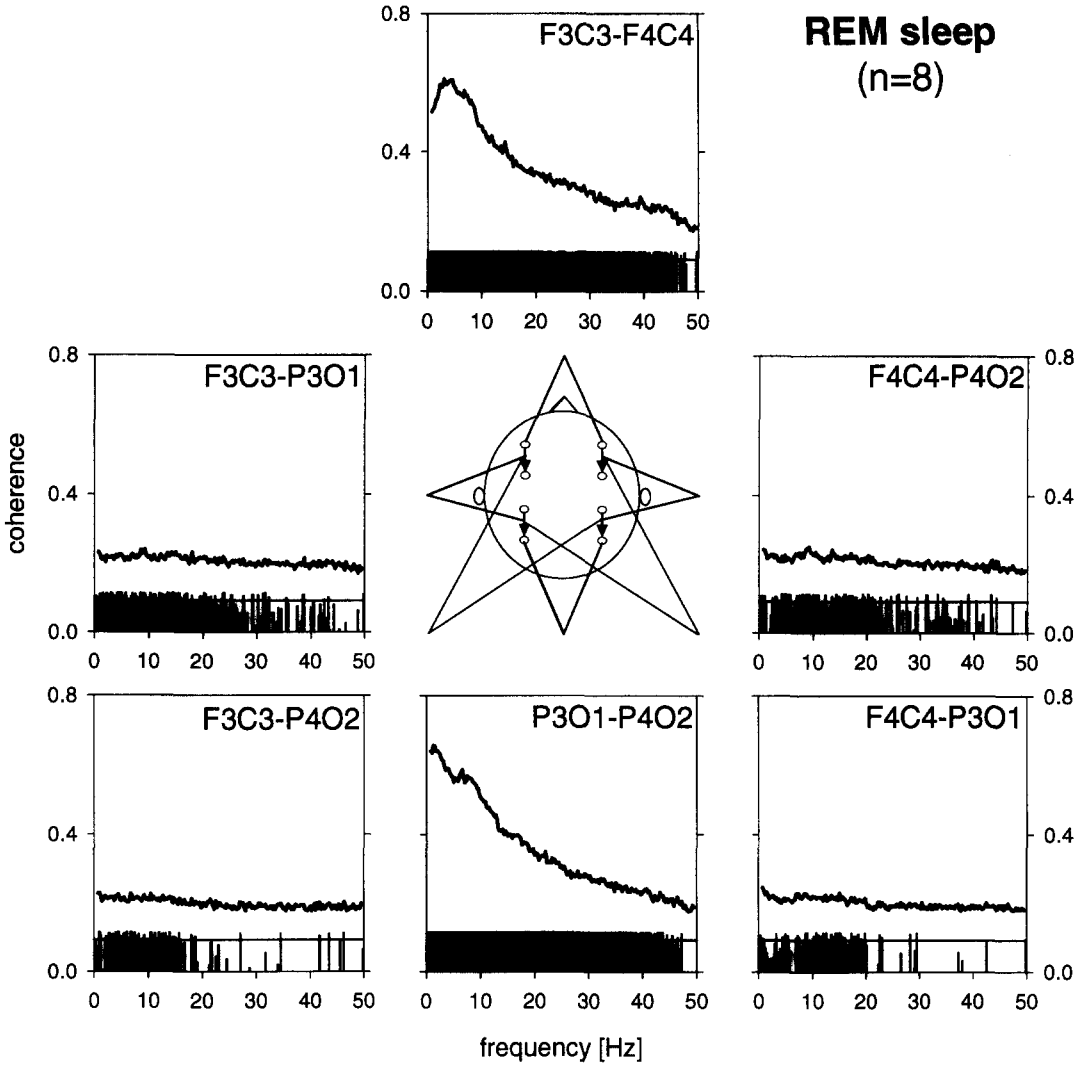

Fig. 5. Mean intrahemispheric and interhemispheric coherence spectra in REM sleep from eight subjects. Middle diagram indicates the pairs of bipolar derivations from which the spectra were calculated. Only 20 s epochs without rapid eye movements were included. On average 121.0 (6.5=S.E.M.) 20 s epochs contributed to a mean spectrum. Significant differences are indicated as in Fig. 4.

coherence was calculated because interhemispheric coherence would have risked to be biased by common electrodes. In Fig. 9 the intrahemispheric coherence spectrum of stage 2 is shown for the usual bipolar derivation and for the CSD derivations calculated from electrodes placed at a similar site. The pattern of the two spectra is very similar.

DISCUSSION

Sleep state-dependent differences

A prominent peak in the coherence of the non-REM sleep EEG was observed in the frequency range of sleep spindles. It dominated the intrahemispheric spectra and was distinct also in the interhemispheric spectra of homologous and non-homologous derivations. These results are consistent with the findings from animal studies that spindles exhibit a synchronized occurrence over large cortical areas as a result of intrinsic properties and connectivity patterns of thalamic neurons.[17] Global coherence of spindle activity was reported to result from corticothalamic projections and not from horizontal intracortical connections.

The dominance of slow-wave activity in the power spectrum of non-REM sleep was not associated with a large peak in the coherence spectrum. Although an elevated level of coherence was invariably present at the low end of the spectra of stage 2 and SWS which generally exceeded the corresponding value of REM sleep, this rise was modest. Moreover, it encompassed only the lowest bins in the delta band, whereas low-frequency power is known to exhibit a state-related modulation over a much larger range (see Ref. 1; Fig. 1). EEG components below 1 Hz which had been originally described in the cat,[47–49,51] were shown to be present also during human sleep.[1,6] Due

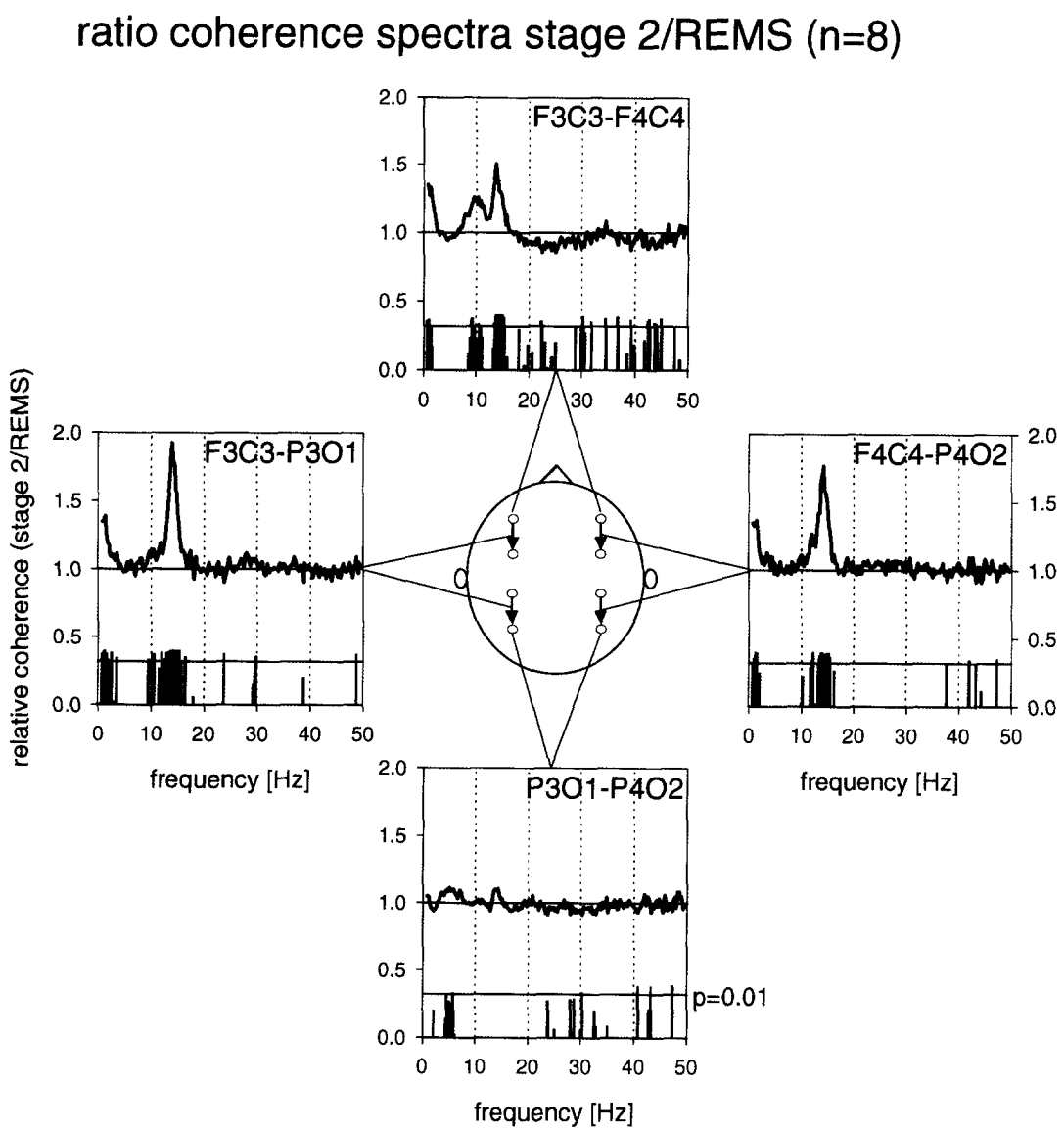

Fig. 6. Intrahemispheric and interhemispheric coherence spectra in stage 2 plotted as a ratio of the corresponding REM sleep value. Mean values from eight subjects (the ratios were calculated for individuals and then averaged). Middle diagram indicates the pairs of bipolar derivations from which the spectra were calculated. Black bars above the abscissae indicate for each bin significant differences between stage 2 and REM sleep (only $P<0.05$ is shown; $1-P$ is plotted on a linear scale; the $P=0.01$ level is indicated and $P=0.05$ corresponds to the abscissa; paired two-tailed t-tests on Fisher's z-transformed coherence values).

to the elimination of the two lowest bins, it was not possible to analyse these components separately in the present study. The increased coherence in the low delta band is consistent with the observation in the cat that slow oscillations are synchronized over wide cortical territories.[5] Moreover, the observation that the values were elevated both in the spindle and low-frequency band, is in agreement with a close association of these two oscillations in the thalamocortical system.

The peak in the alpha band was a prominent feature of the SWS coherence spectra. It exhibited a higher regional specificity than the spindle peak in being largest in the interhemispheric spectrum of the anterior derivations. The alpha-delta pattern is a well known feature of SWS although it is not present in all individuals (for a recent overview, see Ref. 40). It is distinct from alpha activity during waking by its fronto-central and not occipital localization.[43] This is also evident from the high interhemispheric coherence at the anterior derivations. The close functional relationship of alpha and delta activity is underscored by their common enhancement after sleep deprivation.[12,21] It was concluded that this alpha component is associated with sleep-maintaining processes.[40]

Coherence in some parts of the gamma band was higher in REM sleep than in stage 2 or SWS. Bins with significant differences tended to cluster at around 30 Hz in the interhemispheric derivations,

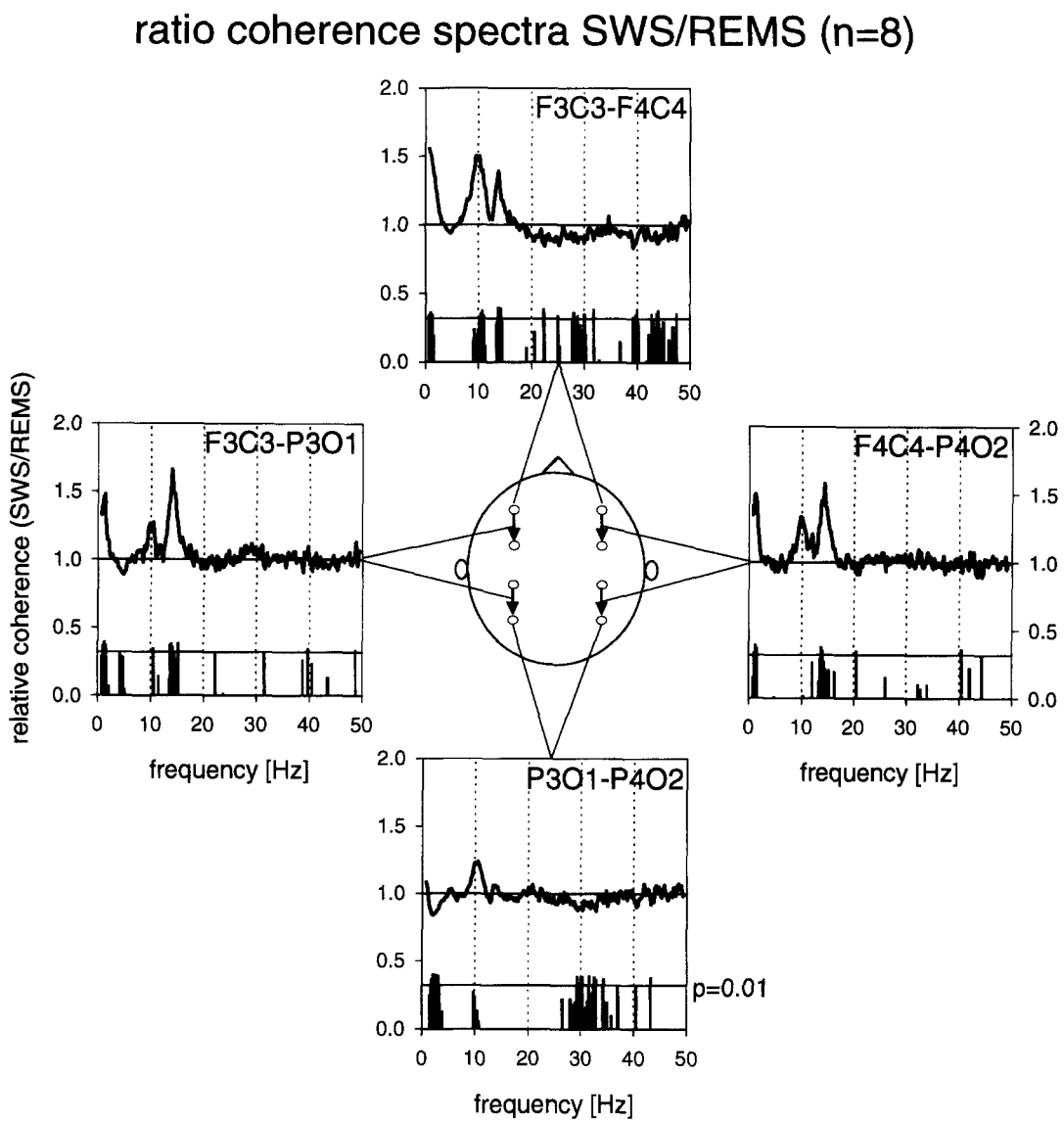

Fig. 7. Intrahemispheric and interhemispheric coherence spectra in slow-wave sleep (SWS) plotted as a ratio of the corresponding REM sleep value. Black bars above the abscissae indicate for each bin significant differences between SWS and REM sleep. For details see Fig. 6.

and at the anterior site also between 39 and 45 Hz. These observations could be related to the MEG findings of Llinás and Ribary[38] that gamma oscillations are more prominent in REM sleep than in SWS. Nevertheless, we are cautious in interpreting these findings in terms of genuine brain potentials because the low amplitude of high-frequency EEG signals carries an increased risk of exhibiting spurious coherences due to small extrinsic signals. Sources of contamination could include minor eye movements which are difficult to identify. A further investigation of these observations is warranted.

Sleep state-independent, regional differences

In both non-REM sleep and REM sleep, the coherence spectra from homologous derivations differed from all other spectra by their high values in the low-frequency range and the marked declining trend from low to high frequencies. The intrahemispheric spectras as well as the "crossed" interhemispheric spectra exhibited a low coherence over the entire spectrum and only a minor frequency-dependent trend. The level of "random coherence" determined by a 20 s displacement of two time series, was reached in the latter already at lower frequencies. The two different patterns are best seen in the REM sleep spectra where peaks are absent (Fig. 5). Confirming and extending previous observations,[24,52] these results constitute strong evidence for a bilateral organization of the basic processes generating the EEG. It is particularly noteworthy that at the low end of the coherence spectra the values for non-REM sleep and REM sleep were at an equally high level,

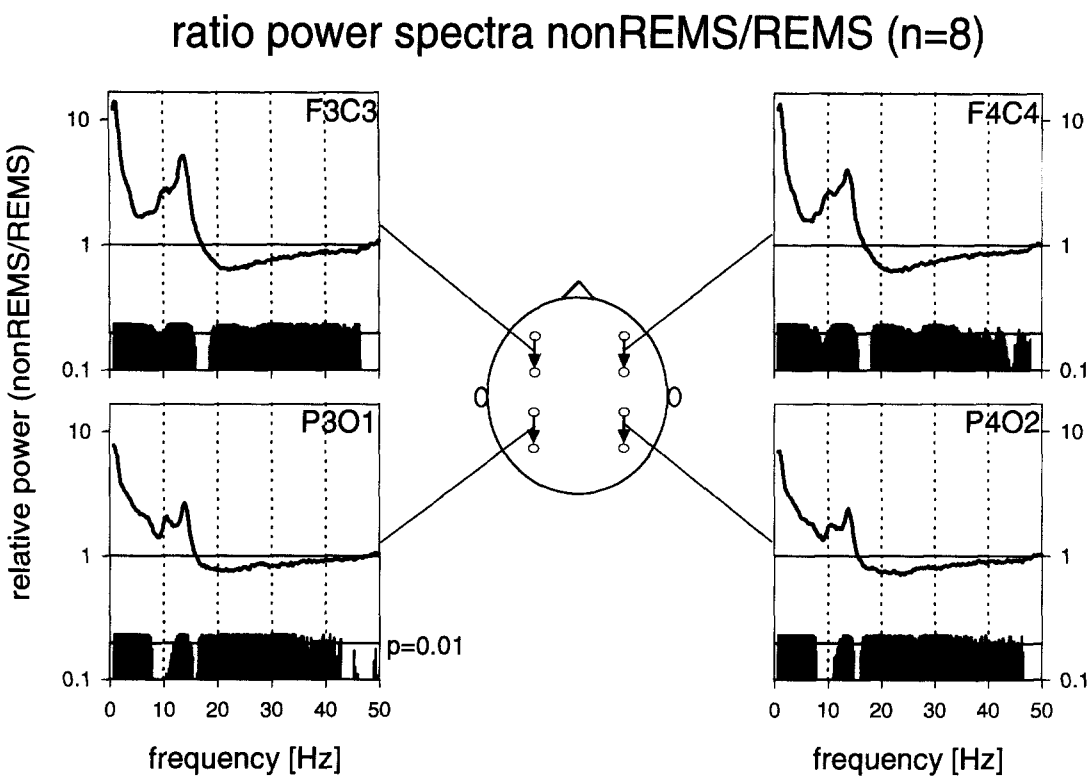

Fig. 8. Power spectra in non-REM sleep (stages 2 to 4) plotted as a ratio of the corresponding REM sleep value. Mean values from eight subjects (the ratios were calculated for individuals and then averaged). Middle diagram indicates the bipolar derivations from which the spectra were calculated. Significant differences are indicated as in Fig. 6.

although their power differed by an order of magnitude (Fig. 8). This supports the conclusion of Bullock *et al.*[13] that "most of the EEG most of the time is not obviously rhythmic" and that the state-dependent oscillations account for only a fraction of the whole energy of the wideband EEG. The marked frequency-dependent change of interhemispheric coherence from homologous derivations resembles the 1/f type of decline in the power spectra, a pattern that is similar for the various sleep stages (Fig. 2). This pattern could be accounted for by a frequency dependent decline of the signal-to-noise ratio in the EEG signal. Assuming that the state-independent part of the EEG consists of a "signal component" with high interhemispheric coherence largely due to transcallosal connectivity, and of a "noise component" arising in the local circuitry with low interhemispheric coherence, the observed coherence pattern would be expected to occur. The involvement of transcallosal pathways is supported by studies in acallosal children in whom the interhemispheric coherence in the low-frequency range was reduced compared to controls.[33,35]

Methodological considerations

It is important to realize that the analysis based on scalp recordings provides information on large scale coherence over a distance of many centimeters and that it can not provide a resolution of finer activity structures. The latter has been investigated by subdural recordings from epileptic patients in which rows of closely spaced electrodes were used.[13,14] The studies revealed that coherence declines with increasing distance between electrode pairs in the millimeter domain, and that this decline is similar for different frequency bands. State related differences in coherence were observed but were inconsistent. There was a tendency of correlated fluctuations across frequency bands. The authors point out that their results obtained with closely spaced subdural electrodes could not predict the large scale coherence between scalp electrodes which are likely to reveal macrostructures.

Coherence is influenced by the electrode configuration and the inter-electrode distance.[28] The present analysis was based on equally spaced bipolar derivations. Common reference electrodes were avoided because they are known to yield either inflated or deflated coherence data.[27] Bipolar recordings from closely spaced electrodes are supposed to reflect the activity of a relatively small area and are an estimate of the first spatial derivative along the vector defined by the interelectrode line. The CSD recording provides an estimate of the second spatial derivative which is perpendicular to the scalp. In a comparison of the two methods for stage 2, similar results were obtained (Fig. 9). Nevertheless, it is

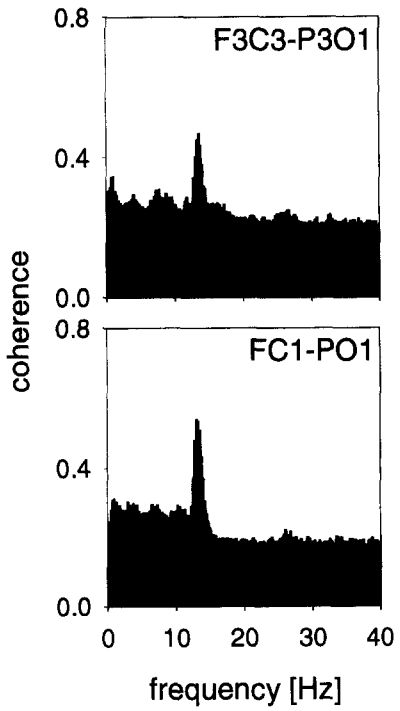

Fig. 9. Average intrahemispheric coherence spectra of bipolar derivations (F3C3−P3O1) and of current source density (CSD) approximations (FC1−PO1) for stage 2 of an individual (609 20 s epochs).

important to keep in mind that all bipolar electrodes were positioned along the antero-posterior axis and that direction sensitivity was not systematically explored.

CONCLUSIONS

The picture emerging from the present analysis is that of two basic sleep states, the one formed by stages 2–4 of non-REM sleep, the other by REM sleep and stage 1. In non-REM sleep three coherent oscillations are superimposed upon basic coherence patterns which are shared by all sleep states. The most prominent oscillations are those of sleep spindles whose dominant frequency exhibits a high degree of intra-individual stability within and across sleep episodes and which occur at a 4/s periodicity.[1,26] The coherence peak of the present study occurred at 13–14 Hz whereas the low-frequency spindles at 11–12 Hz[58] were not very conspicuous in the coherence spectra. Nevertheless, a small significant peak was present in the intrahemispheric spectra (Fig. 6). The observation that spindles induce periodically a short-lasting, highly coherent activity throughout the cortex raises the question whether they are of functional significance for sleep. Should they be regarded as carrier frequencies upon which some relevant information is modulated? Although such considerations are presently purely speculative, waking-related information is known to be manifested during sleep in animals. Thus in the rat, the correlated activity of hippocampal place cells during non-REM sleep reflects the activity of those cells during spatial exploration in the preceding waking state.[59] These re-activated correlated states appear during hippocampal sharp waves and are reduced or absent in the intervals between these events.[44] As pointed out by Buzsáki and Chrobak,[15] oscillations of neural networks may be instrumental for synchronizing the activity of anatomically distributed populations of neurons. The authors propose that they may provide the precise temporal structure for ensembles of neurons to perform specific functions, including sensory binding and memory formation. They consider that each sharp wave burst in the hippocampus may reflect a fast "replay" of recent network modifications. Contreras and Steriade[16] hypothesize that the synchronized depolarizing phases of slow oscillations generate cyclic spike trains that "may serve to reinforce/specify the neuronal circuitry and to subserve a lengthy persistence of information acquired during wakefulness through internally generated "non-utilitarian" excitations occurring during the state of sleep"... As a counterpart of slow-waves and spindles, coherent high frequency components seem to prevail during the cortically-activated sleep states. Recordings using more sensitive techniques than the EEG have demonstrated a prominent coherent high-frequency activity during REM sleep which has been related to dreaming.[38] It is tempting to speculate that the different state-specific coherent oscillations may subserve specific functions in sleep.

Acknowledgements—We thank Dr Hans-Ruedi Künsch for statistical advise in coherence calculations and Dr Irene Tobler for comments on the manuscript. The study was supported by the Swiss National Science Foundation grant 3100-042500.94 and the Human Frontiers Science Program grant RG-81/96.

REFERENCES

1. Achermann P. and Borbély A. A. (1997) Low-frequency (<1Hz) oscillations in the human sleep EEG. *Neuroscience* **81,** 213–222.
2. Achermann P., Dijk D. J., Brunner D. P. and Borbély A. A. (1993) A model of human sleep homeostasis based on EEG slow-wave activity: quantitative comparison of data and simulations. *Brain Res. Bull.* **31,** 97–113.
3. Aeschbach D. and Borbély A. A. (1993) All-night dynamics of the human sleep EEG. *J. Sleep Res.* **2,** 70–81.
4. Aeschbach D., Dijk D. J. and Borbély A. A. (1997) Dynamics of EEG spindle frequency activity during extended sleep in humans: relationship to slow-wave activity and time of day. *Brain Res.* **748,** 131–136.
5. Amzica F. and Steriade M. (1995) Short- and long-range neuronal synchronization of the slow (<1Hz) cortical oscillation. *J. Neurophysiol.* **73,** 20–38.

6. Amzica F. and Steriade M. (1997) The K-complex: its slow (<1 Hz) rhythmicity and relation with delta waves. *Neurology* **49,** 952–959.
7. Banquet J. P. (1983) Inter- and intrahemispheric relationships of the EEG activity during sleep in man. *Electroenceph. clin. Neurophysiol.* **55,** 51–59.
8. Barcaro U., Denoth F., Murri L., Navona C. and Stefanini A. (1986) Changes in the interhemispheric correlation during sleep in normal subjects. *Electroenceph. clin. Neurophysiol.* **63,** 112–118.
9. Benington J. H. and Heller H. C. (1995) Restoration of brain energy metabolism as the function of sleep. *Prog. Neurobiol.* **45,** 347–360.
10. Borbély A. A. (1982) A two process model of sleep regulation. *Hum. Neurobiol.* **1,** 195–204.
11. Borbély A. A. and Achermann P. (1992) Concepts and models of sleep regulation: an overview. *J. Sleep Res.* **1,** 63–79.
12. Borbély A. A., Baumann F., Brandeis D., Strauch I. and Lehmann D. (1981) Sleep deprivation: effect on sleep stages and EEG power density in man. *Electroenceph. clin. Neurophysiol.* **51,** 483–495.
13. Bullock T. H., McClune M. C., Achimowicz J. Z., Iragui-Madoz V. J., Duckrow R. B. and Spencer S. S. (1995) EEG coherence has structure in the millimeter domain: subdural and hippocampal recordings from epileptic patients. *Electroenceph. clin. Neurophysiol.* **95,** 161–177.
14. Bullock T. H., McClune M. C., Achimowicz J. Z., Iragui-Madoz V. J., Duckrow R. B. and Spencer S. S. (1995) Temporal fluctuations in coherence of brain waves. *Proc. natn. Acad. Sci. U.S.A.* **92,** 11,568–11,572.
15. Buzsáki G. and Chrobak J. J. (1995) Temporal structure in spatially organized neuronal ensembles: a role for interneuronal networks. *Curr. Opin. Neurobiol.* **5,** 504–510.
16. Contreras D. and Steriade M. (1995) Cellular basis of EEG slow rhythms: a study of dynamic corticothalamic relationships. *J. Neurosci.* **15,** 604–622.
17. Contreras D., Destexhe A., Sejnowski T. J. and Steriade M. (1996) Control of spatiotemporal coherence of a thalamic oscillation by corticothalamic feedback. *Science* **274,** 771–774.
18. Contreras D., Destexhe A., Sejnowski T. J. and Steriade M. (1997) Spatiotemporal patterns of spindle oscillations in cortex and thalamus. *J. Neurosci.* **17,** 1179–1196.
19. Daan S., Beersma D. G. M. and Borbély A. A. (1984) Timing of human sleep: recovery process gated by a circadian pacemaker. *Am. J. Physiol.* **246,** R161–R183.
20. Dijk D. J. and Czeisler C. A. (1995) Contribution of the circadian pacemaker and the sleep homeostat to sleep propensity, sleep structure, electroencephalographic slow waves, and sleep spindle activity in humans. *J. Neurosci.* **15,** 3526–3538.
21. Dijk D. J., Brunner D. P. and Borbély A. A. (1990) Time course of EEG power density during long sleep in humans. *Am. J. Physiol.* **258,** R650–R661.
22. Dijk D. J., Brunner D. P., Beersma D. G. M. and Borbély A. A. (1990) Slow wave sleep and electroencephalogram power density as a function of prior waking and circadian phase. *Sleep* **13,** 430–440.
23. Dijk D. J., Hayes B. and Czeisler C. A. (1993) Dynamics of electroencephalographic sleep spindles and slow wave activity in men: effect of sleep deprivation. *Brain Res.* **626,** 190–199.
24. Dumermuth G., Walz W., Scollo-Lavizzari G. and Kleiner B. (1972) Spectral analysis of EEG activity in different sleep stages in normal adults. *Eur. Neurol.* **7,** 265–296.
25. Dumermuth G., Lange B., Lehmann D., Meier C. A., Dinkelmann R. and Molinari L. (1983) Spectral analysis of all-night sleep EEG in healthy adults. *Eur. Neurol.* **22,** 322–339.
26. Evans B. M. and Richardson N. E. (1995) Demonstration of a 3–5s periodicity between the spindle bursts in NREM sleep in man. *J. Sleep Res.* **4,** 196–197.
27. Fein G., Raz J., Brown F. F. and Merrin E. L. (1988) Common reference coherence data are confounded by power and phase effects. *Electroenceph. clin. Neurophysiol.* **69,** 581–584.
28. French C. C. and Beaumont J. G. (1984) A critical review of EEG coherence studies of hemisphere function. *Int. J. Psychophysiol.* **1,** 241–254.
29. Hirsch J. C., Fourment A. and Marc M. E. (1983) Sleep-related variations of membrane potential in the lateral geniculate body relay neurons of the cat. *Brain Res.* **259,** 308–312.
30. Hjorth B. (1975) An on-line transformation of EEG scalp potentials into orthogonal source derivations. *Electroenceph. clin. Neurophysiol.* **39,** 526–530.
31. Kaminski M., Blinowska K. and Szelenberger W. (1997) Topographic analysis of coherence and propagation of EEG activity during sleep and wakefulness. *Electroenceph. clin. Neurophysiol.* **102,** 216–227.
32. Kattler H., Dijk D. J. and Borbély A. A. (1994) Effect of unilateral somatosensory stimulation prior to sleep on the sleep EEG in humans. *J. Sleep Res.* **3,** 159–164.
33. Koeda T., Knyazeva M., Njiokiktjien C., Jonkman E. J., De Sonneville L. and Vildavsky V. (1995) The EEG in acallosal children. Coherence values in the resting state: left hemisphere compensatory mechanism? *Electroenceph. clin. Neurophysiol.* **95,** 397–407.
34. Krueger J. M. and Obál F. (1993) A neuronal group theory of sleep function. *J. Sleep Res.* **2,** 63–69.
35. Kuks J. B. M., Vos J. E. and O'Brien M. J. (1987) Coherence patterns of the infant sleep EEG in absence of the corpus callosum. *Electroenceph. clin. Neurophysiol.* **66,** 8–14.
36. Lagerlund T. D., Sharbrough F. W., Busacker N. E. and Cicora K. M. (1995) Interelectrode coherences from nearest-neighbor and spherical harmonic expansion computation of laplacian of scalp potential. *Electroenceph. clin. Neurophysiol.* **95,** 178–188.
37. Leuchter A. F., Dunkin J. J., Lufkin R. B., Anzai Y., Cook I. A. and Newtin T. F. (1994) Effect of white matter disease on functional connections in the aging brain. *J. Neurol. Neurosurg. Psychiat.* **57,** 1347–1354.
38. Llinás R. and Ribary U. (1993) Coherent 40Hz oscillation characterizes dream state in humans. *Proc. natn. Acad. Sci. U.S.A.* **90,** 2078–2081.
39. Nielsen T., Abel A., Lorrain D. and Montplaisir J. (1990) Interhemispheric EEG coherence during sleep and wakefulness in left- and right-handed subjects. *Brain Cogn.* **14,** 113–125.
40. Pivik R. T. and Harman K. (1995) A reconceptualization of EEG alpha activity as an index of arousal during sleep: all alpha activity is not equal. *J. Sleep Res.* **4,** 131–137.

41. Priestley M. B. (1981) *Spectral Analysis and Time Series*, Vol. 2, *Multivariate Series, Prediction and Control.* Academic, New York.
42. Rechtschaffen A. and Kales A. (1968) *A Manual of Standardized Terminology, Techniques and Scoring System for Sleep Stages of Human Subjects.* UCLA Brain Information Service: Brain Research Institute, Los Angeles.
43. Scheuler W., Stinshoff D. and Kubicki S. (1983) The alpha-sleep pattern: differentiation from other sleep patterns and effect of hypnotics. *Neuropsychobiology* **10,** 183–189.
44. Shen B. and McNaughton B. L. (1996) Modeling the spontaneous reactivation of experience-specific hippocampal cell assembles during sleep. *Hippocampus* **6,** 685–692.
45. Steriade M., Jones E. G. and Llinás R. R. (1990) *Thalamic Oscillations and Signaling.* Wiley, New York.
46. Steriade M., McCormick D. A. and Sejnowski T. J. (1993) Thalamocortical oscillations in the sleeping and aroused brain. *Science* **262,** 679–685.
47. Steriade M., Nuñez A. and Amzica F. (1993) A novel low (<1Hz) oscillation of neurocortical neurons *in vivo*: depolarizing and hyperpolarizing components. *J. Neurosci.* **13,** 3252–3265.
48. Steriade M., Nuñez A. and Amzica F. (1993) Intracellular analysis of relations between the slow (<1Hz) neocortical oscillation and other sleep rhythms of the electroencephalogram. *J. Neurosci.* **13,** 3266–3283.
49. Steriade M., Contreras D., Curro Dossi R. and Nuñez A. (1993) The slow (<1Hz) oscillation in reticular thalamic and thalamocortical neurons: scenario of sleep rhythm generation in interacting thalamic and neocortical networks. *J. Neurosci.* **13,** 3284–3299.
50. Steriade M., Contreras D. and Amzica F. (1994) Synchronized sleep oscillations and their paroxysmal developments. *Trends Neurosci.* **17,** 199–208.
51. Steriade M., Amzica F. and Contreras D. (1996) Synchronization of fast (30–40Hz) spontaneous cortical rhythms during brain activation. *J. Neurosci.* **16,** 392–417.
52. Terstegge K., Henkes H., Scheuler W., Hansen M. L., Ruf B. and Kubicki St. (1993) Spectral power and coherence analysis of sleep EEG in AIDS patients: decrease in interhemispheric coherence. *Sleep* **16,** 137–145.
53. Wallin G. and Stalberg E. (1980) Source derivation in clinical routine EEG. *Electroenceph. clin. Neurophysiol.* **50,** 282–292.
54. Welch P. D. (1967) The use of fast fourier transform for the estimation of power spectra: a method based on time averaging over short, modified preiodograms. *IEEE Trans. Audio Electroacoust.* **AU-15,** 70–73.
55. Werth E., Achermann P. and Borbély A. A. (1996) Brain topography of the human sleep EEG: antero-posterior shifts of spectral power. *NeuroReport* **8,** 123–127.
56. Werth E., Achermann P. and Borbély A. A. (1997) Fronto-occipital EEG power gradients in human sleep. *J. Sleep Res.* **6,** 102–112.
57. Werth E., Dijk D. J., Achermann P. and Borbély A. A. (1996) Dynamics of the sleep EEG after an early evening nap: experimental data and simulations. *Am. J. Physiol.* **271,** R501–R510.
58. Werth E., Achermann P., Dijk D. J. and Borbély A. A. (1997) Spindle frequency activity in the sleep EEG: individual differences and topographical distribution. *Electroenceph. clin. Neurophysiol.* **103,** 535–542.
59. Wilson M. A. and McNaughton B. L. (1994) Reactivation of hippocampal ensemble memories during sleep. *Science* **265,** 603–604.

(*Accepted* 15 *December* 1997)